Domain wall suppression in trapped mixtures of Bose-Einstein condensates

Francesco V. Pepe,[1,2] Paolo Facchi,[2,3] Giuseppe Florio,[1,2,4] and Saverio Pascazio[1,2]
[1]*Dipartimento di Fisica and MECENAS, Università di Bari, I-70126 Bari, Italy*
[2]*Istituto Nazionale di Fisica Nucleare, Sezione di Bari, I-70126 Bari, Italy*
[3]*Dipartimento di Matematica and MECENAS, Università di Bari, I-70125 Bari, Italy*
[4]*Museo Storico della Fisica e Centro Studi e Ricerche "Enrico Fermi", Piazza del Viminale 1, I-00184 Roma, Italy*
(Received 14 June 2012; published 22 August 2012)

The ground-state energy of a binary mixture of Bose-Einstein condensates can be estimated for large atomic samples by making use of suitably regularized Thomas-Fermi density profiles. By exploiting a variational method on the trial densities the energy can be computed by explicitly taking into account the normalization condition. This yields analytical results and provides the basis for further improvement of the approximation. As a case study, we consider a binary mixture of ^{87}Rb atoms in two different hyperfine states in a double-well potential and discuss the energy crossing between density profiles with different numbers of domain walls, as the number of particles and the interspecies interaction vary.

DOI: 10.1103/PhysRevA.86.023629 PACS number(s): 67.85.Hj, 67.85.Bc, 03.75.Mn

I. INTRODUCTION

Binary mixtures of Bose-Einstein condensates [1] are of great interest due to their complex dynamical features and their role in the emergence of macroscopic quantum phenomena [2]. Mixtures are experimentally available and usually made up of two alkali atomic species [3–9]. They generally display repulsive self-interaction and are confined by various external potentials. Depending on the interspecies interaction, two classes of stable configurations are possible: mixed and separated. The latter are more interesting, since it is in this case that the observation of phenomena such as symmetry breaking and macroscopic quantum tunneling of one species through the other one [10–12] is possible. Evidence of phase separation has been observed in Refs. [8,9]. Many recent articles are devoted to the investigation of dynamical effects in mixtures, such as vortices and solitons (see [13–16] for recent experimental and theoretical studies).

Different approaches are possible in order to study the ground state of these systems. If the number of particles in the condensate is very large compared to the number of particles in the excited states, the fields associated to the two species can be treated as classical wave functions. This approach leads to the Gross-Pitaevskii equations [17], which are nonlinear Schrödinger equations obtained by finding stationary points of the zero-temperature grand-canonical energy of the system. The Thomas-Fermi (TF) approximation, which consists in this case in neglecting the kinetic energy of the system, is then usually applied [17]. A great deal of results are obtained in particular cases, such as confinement by a hard wall trap [18], harmonic or lattice potentials [19], and axisymmetric traps [20], and also in the presence of the gravitational force [21]. The problem of the stability of mixtures has been tackled also with renormalization-group techniques [22].

The presence of the kinetic term in the energy functional of a binary mixture leads in particular to the regularization of possible domain walls, which sharply separate the two species in the TF ground states [10,23–26]. This is generally related to the problem of minimizing the surface energy, that is also found in the theory of superconductivity [27].

In this work we introduce a variational method in order to approximate the Gross-Pitaevskii solution in a neighborhood of a domain wall and estimate the total energy of a mixture. Our technique explicitly takes into account the normalization of the condensate wave functions and ensures complete analytical feasibility.

This article is organized as follows: in Sec. II we summarize results obtained in the TF approximation which are relevant to our analysis; in Sec. III we introduce the regularization technique and obtain results regarding the energy increase with respect to the TF approximation; in Sec. IV we examine a case study in which macroscopic effects related to domain-wall suppression can be observed and present a quantitative phase diagram; in Sec. V we suggest further possible developments of our technique.

II. BINARY MIXTURES

A. Energy functional

Let us consider a binary mixture of Bose-Einstein condensates, confined by the external potentials $V_k(x)$, with $k = 1,2$. We assume that the particles are tightly confined in the transverse directions, so that the system is quasi-one-dimensional [17]. Let $U_{kk} > 0$ be the parameters that determine the self-interaction between particles of each species and $U_{12} = U_{21} > 0$ be the interspecies interaction parameter. The ground state of the system is determined by the coupled Gross-Pitaevskii equations [17,27,28]

$$\left\{ -\frac{\hbar^2}{2m_k}\frac{d^2}{dx^2} + V_k(x) + \sum_j U_{kj}|\psi_j(x)|^2 - \mu_k \right\}\psi_k(x) = 0, \tag{1}$$

with $k = 1,2$. They are the variational equations of the quartic energy functional

$$\mathcal{E}(\psi_1,\psi_2) = \sum_k \{\mathcal{T}_k(\psi_k) + \mathcal{V}_k(\psi_k)\} + \mathcal{U}(\psi_1,\psi_2) \tag{2}$$

under the constraints

$$\int dx\, \rho_k(x) = N_k, \tag{3}$$

where

$$\begin{aligned} \mathcal{T}_k(\psi_k) &= \int \frac{\hbar^2}{2m_k} \left| \frac{d\psi_k}{dx}(x) \right|^2 dx, \\ \mathcal{V}_k(\psi_k) &= \int V_k(x) |\psi_k(x)|^2 dx, \\ \mathcal{U}(\psi_1, \psi_2) &= \sum_{j,k} \mathcal{U}_{jk}(\psi_j, \psi_k) \\ &= \frac{1}{2} \sum_{j,k} \int U_{jk} |\psi_j(x)|^2 |\psi_k(x)|^2 dx. \end{aligned} \tag{4}$$

Here $\psi_k(x)$ are the condensate wave functions, whose squared moduli $\rho_k(x) = |\psi_k(x)|^2$ represent the local densities of each species; N_k are the numbers of particles making up the condensates; while $\mathcal{T}_k$, $\mathcal{V}_k$, and $\mathcal{U}$ are the kinetic, potential, and interaction energy, respectively. We will assume henceforth that the condensate wave functions are real, since energy minimization requires their phases to be constant.

B. Thomas-Fermi approximation

The TF approximation [17] is in this case equivalent to neglecting the kinetic terms in Eqs. (1) and (2), so that

$$\mathcal{E}_{\mathrm{TF}}(\rho_1, \rho_2) = \sum_k \mathcal{V}_k(\sqrt{\rho_k}) + \mathcal{U}(\sqrt{\rho_1}, \sqrt{\rho_2}). \tag{5}$$

The value of the adimensional parameter

$$\alpha = \frac{U_{12}}{\sqrt{U_{11} U_{22}}} \tag{6}$$

is crucial in qualitatively determining the TF ground state. If $\alpha > 1$, which is the case of interest here, the ground-state density profiles are completely separated in adjacent regions divided by domain walls. In the regions where only species k is present, the solution to the TF equations reads

$$\rho_k^{\mathrm{TF}}(x) = \frac{\mu_k - V_k(x)}{U_{kk}}. \tag{7}$$

Equation (7) completely determines the functional dependence of the densities on the external potential (and on the chemical potentials), once their supports are given. Here we are interested in the ground-state solution, so that the supports are determined by minimizing the energy of the system Eq. (2) as a function of the number and the positions of the domain walls. In Ref. [29] we proved that for continuous trapping potentials stationarity of energy requires that the densities at a domain wall at R_j satisfy

$$\sqrt{U_{11}} \rho_1(R_j) = \sqrt{U_{22}} \rho_2(R_j). \tag{8}$$

Moreover, in the special case $V(x) \equiv V_1(x) = V_2(x)$, conditions Eq. (8) imply that the external potential, and thus the density of each species, should be the same at all domain walls.

The TF approximation works very well for large numbers of particles and provides a good estimate of the energy of the system. Despite being small with respect to the potential energy, corrections due to the kinetic term nonetheless give rise to macroscopic effects. The most relevant of such effects is the crossing between stationary states with different numbers of domain walls in the ground state [11,12]. It is thus necessary, in order to determine the actual ground state of a mixture, to consider a regularization scheme of the TF density profiles, that enables us to smooth parts of the TF profiles, like domain walls and zeros, that provide an infinite contribution to the kinetic energy [17].

III. VARIATIONAL REGULARIZATION OF DENSITY PROFILES

Many attempts have been made so far in order to consistently estimate the energy corrections due to the kinetic contribution. The pioneering works by Ao and Chui [10] and Timmermans [23] are based on an exponential approximation of the TF density profiles, by extrapolating the solution of the Gross-Pitaevskii equations far from a domain wall, and on a linear approximation of the regularized walls, respectively. Other authors [24,26] put forward a regularization with fixed chemical potential in various regimes.

The task we will try to accomplish in this work is to find a proper domain-wall regularization, which provides a reliable approximation to the ground-state profile and energy of a binary mixture in a trapping potential, and which is at the same time an analytically manageable trial function. The approximations in Refs. [10,23] are based on a rather crude ansatz, but provide a good estimation of the order of magnitude of the energy changes due to the kinetic terms. However, we will try to find better upper bounds to the ground-state energies, since it is possible that a small energy change results in macroscopic differences in density profiles. Our approximation will be referred to a system with fixed numbers of particles, and will strictly rely on the preservation of the normalization conditions. It is indeed difficult to use results obtained with a fixed chemical potential [24,26] in this case, since for nontrivial external potentials it is generally impossible to invert the normalization conditions in Eq. (3) and explicitly express the chemical potentials as functions of the numbers of particles.

A. Domain walls

In order to regularize the domain walls, it is sufficient to replace the singular TF density profiles with a continuous function, with a bounded first derivative. The minimization of the kinetic energy leads to tails of each species penetrating through the domain wall.

Our choice of trial profiles is based on an exponential tail regularization of the TF solutions. Let us consider a domain wall placed at position R_0. In its neighborhood we assume as profiles the continuous functions

$$\tilde{\rho}_1(x) = \begin{cases} \rho_1^{\mathrm{TF}}(x) & \text{if} \quad x < R_1 \\ \rho_1^{\mathrm{TF}}(R_1) \mathrm{e}^{-2(x-R_1)/\Lambda_1} & \text{if} \quad x \geqslant R_1 \end{cases}, \tag{9}$$

and

$$\tilde{\rho}_2(x) = \begin{cases} \rho_2^{\mathrm{TF}}(x) & \text{if} \quad x > R_2 \\ \rho_2^{\mathrm{TF}}(R_2) \mathrm{e}^{2(x-R_2)/\Lambda_2} & \text{if} \quad x \leqslant R_2 \end{cases}, \tag{10}$$

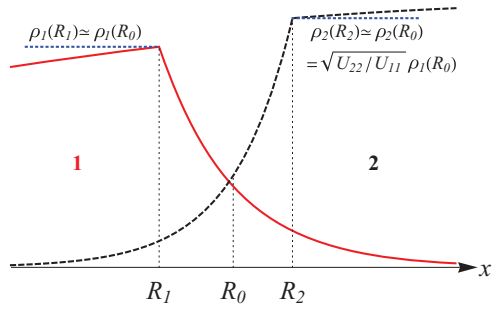

FIG. 1. (Color online) Plot of the trial density profiles Eqs. (9) and (10) in a neighborhood of a domain wall placed at R_0. The solid (red) line represents the density of the first species, and the dashed (black) line represents the density of the second species, with $U_{11} < U_{22}$.

with $R_1 < R_0 < R_2$, $\Lambda_k > 0$, and $\rho_k^{\rm TF}$ being the TF densities Eq. (7). See Fig. 1. The points R_k are fixed in order to locally preserve the normalization conditions. This is accomplished by imposing that the integral of the removed part of the TF profiles be equal to that of the new exponential tails:

$$\int_{R_k}^{R_0} dx\, \rho_k^{\rm TF}(x) = \int_{R_k}^{(-1)^{k+1}\infty} dx\, \tilde{\rho}_k(x), \tag{11}$$

which gives

$$R_k - R_0 = (-1)^k \frac{\Lambda_k}{2}\left\{1 + {\rm O}\left[\Lambda_k \frac{\rho_k^{\rm TF\prime}(R_0)}{\rho_k^{\rm TF}(R_0)}\right]\right\}. \tag{12}$$

In the following, we will neglect all corrections depending on the first derivatives of the TF densities, $\rho_k^{\rm TF\prime} = d\rho_k^{\rm TF}/dx$, which depend linearly on the derivatives of the external potentials. This assumption, which involves conditions on the (by now arbitrary) parameters Λ_k, will be expressed at the end of our calculations in term of physical quantities. It is remarkable that under this approximation the regularized density profiles still satisfy condition Eq. (8) at R_0.

Once the trial profiles are chosen, we proceed to the computation of the difference in potential and interaction energy with respect to the TF densities. It is convenient to explicitly show the dependence of the energy on the largest penetration length, say Λ_1, and the ratio $\eta = \Lambda_2/\Lambda_1 \leqslant 1$. Since $\alpha > 1$, the mixing must result in an increase in potential energy. The self-interaction energy associated to the exponential tail of $\tilde{\rho}_1(x)$ reads

$$\tilde{\mathcal{U}}_{11} = \frac{U_{11}}{2}\int_{R_1}^{\infty} \tilde{\rho}_1(x)\,dx = \frac{1}{8}\Lambda_1\left[\rho_1^{\rm TF}(R_0)\right]^2. \tag{13}$$

This contribution replaces the self-interaction energy of the removed TF density:

$$\mathcal{U}_{11}^{\rm TF} = \frac{U_{11}}{2}\int_{R_1}^{R_0} \rho_1^{\rm TF}(x)\,dx = \frac{1}{4}\Lambda_1\left[\rho_1^{\rm TF}(R_0)\right]^2. \tag{14}$$

The same results hold for the second species after the substitution $\Lambda_1 \to \eta\Lambda_1$. As expected, extending the density profiles implies a reduction in the self-interaction energy, $\mathcal{U}_{\rm self} = \mathcal{U}_{11} + \mathcal{U}_{22}$, which reads

$$\Delta\mathcal{U}_{\rm self}(\Lambda_1,\eta) = -\tfrac{1}{8}(1+\eta)U_{11}\Lambda_1\left[\rho_1^{\rm TF}(R_0)\right]^2. \tag{15}$$

A positive contribution comes from the interspecies interaction terms, $\mathcal{U}_{\rm inter} = \mathcal{U}_{12} + \mathcal{U}_{21}$, which are due to the penetration of the tails in the bulk of the other species and their superposition around R_0. (Remember that in a TF separated configuration $\mathcal{U}_{\rm inter} = 0$.) The total change in the interspecies interaction energy reads

$$\begin{aligned}\mathcal{U}_{\rm inter}(\Lambda_1,\eta) &= U_{12}\int_{-\infty}^{\infty} \tilde{\rho}_1(x)\tilde{\rho}_2(x)\,dx \\ &= \frac{\alpha U_{11}\Lambda_1[{\rm e}^{-(1+\eta)} - \eta^2{\rm e}^{-(1+1/\eta)}]}{2(1-\eta)}\left[\rho_1^{\rm TF}(R_0)\right]^2.\end{aligned} \tag{16}$$

Observe that the limit $\eta \to 1$ is finite. It is easy to verify that no corrections come from the interaction with the external potential at the chosen order of approximation. The results Eqs. (15) and (16) are found under the hypothesis that the distance separating the considered domain wall from other possible walls is much larger than the Λ_k's.

Let us now consider the contributions from the kinetic energy. The value of the kinetic energy of the densities in the bulk is consistently neglected in our approximation, being ${\rm O}[(\Lambda_k\rho_k^{\rm TF\prime}/\rho_k^{\rm TF})^2]$ with respect to the leading terms. On the other hand, the contribution across the domain wall depends on the inverse penetration lengths and reads

$$\begin{aligned}\mathcal{T}_{\rm wall}(\Lambda_1,\eta) &= \frac{\hbar^2}{2m_1}\int_{R_1}^{+\infty}\left|\frac{d\sqrt{\tilde{\rho}_1}}{dx}\right|^2 dx \\ &\quad + \frac{\hbar^2}{2m_2}\int_{-\infty}^{R_2}\left|\frac{d\sqrt{\tilde{\rho}_2}}{dx}\right|^2 dx \\ &= \frac{\hbar^2}{4m_1\Lambda_1}\left(1+\frac{\eta_0^2}{\eta}\right)\rho_1^{\rm TF}(R_0),\end{aligned} \tag{17}$$

where

$$\eta_0 \equiv \frac{\xi_2}{\xi_1} = \left(\frac{m_1}{m_2}\right)^{\frac{1}{2}}\left(\frac{U_{11}}{U_{22}}\right)^{\frac{1}{4}} \tag{18}$$

is the ratio between the healing lengths

$$\xi_k = \hbar/\sqrt{2m_k U_{kk}\rho_k^{\rm TF}(R_0)}, \tag{19}$$

($k = 1,2$) of uniform condensates whose densities are $\rho_k^{\rm TF}(R_0)$ [17].

The energetic contributions Eqs. (15)–(17) depend on the free parameters Λ_k. Heuristically, as a benchmark, one can evaluate them at $\Lambda_k = \xi_k/\sqrt{\alpha-1}$, the penetration lengths associated with the exponential tail of one species into the bulk of the other one, which are obtained via an approximated Gross-Pitaevskii equation [10]. Besides yielding a divergence of the penetration for α close to 1, which is unphysical for a system with a finite numbers of particles, this is not the optimal choice, and it can even yield an energy 20% larger than the minimum for physical parameters. In a situation where small energy changes are involved, this discrepancy can be very relevant. The best strategy is to minimize the total energy of the wall over the family of trial functions Eqs. (9) and (10) parametrized by Λ_1 and $\eta = \Lambda_2/\Lambda_1$:

$$\mathcal{E}_{\rm wall}(R_0) = \min_{\Lambda_1,\eta}\left\{\Delta\mathcal{U}_{\rm self} + \mathcal{U}_{\rm inter} + \mathcal{T}_{\rm wall}\right\}. \tag{20}$$

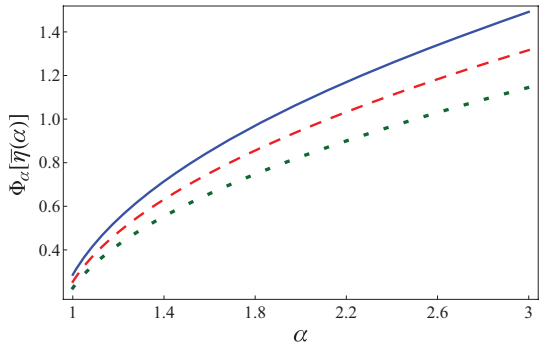

FIG. 2. (Color online) Behavior of the function $\Phi_\alpha[\bar\eta(\alpha)]$, obtained by solving Eq. (23), for different values of η_0. Solid (blue) line, $\eta_0 = 0.99$; dashed (red) line, $\eta_0 = 0.75$; dotted (green) line, $\eta_0 = 0.5$.

This will enable us to get a much more accurate upper bound for the ground-state energy of the binary mixture.

The minimum in Eq. (20) is attained at a single point $[\bar\Lambda_1(\alpha), \bar\eta(\alpha)]$ and reads

$$\mathcal{E}_{\rm wall}(R_0) = \left\{\frac{\hbar^2 U_{11}\left[\rho_1^{\rm TF}(R_0)\right]^3}{2m_1}\right\}^{\frac{1}{2}} \Phi_\alpha[\bar\eta(\alpha)], \tag{21}$$

where

$$\Phi_\alpha(\eta) = \left\{\alpha\frac{[\mathrm{e}^{-(1+\eta)} - \eta^2\mathrm{e}^{-(1+1/\eta)}]}{1-\eta} - \frac{1+\eta}{4}\right\}^{1/2} \times \left(1+\frac{\eta_0^2}{\eta}\right)^{1/2}. \tag{22}$$

The optimal ratio between the penetration lengths, $\bar\eta(\alpha)$, is the solution to the transcendental equation:

$$\mathrm{e}^{\eta}\left[\mathrm{e}^{1+1/\eta}(1-\eta)^2\left(\eta^2-\eta_0^2\right) + 4\alpha\,\eta\left(\eta+\eta^2-\eta^3+\eta_0^2\right)\right] = 4\alpha\,\mathrm{e}^{1/\eta}\left[\eta^3 - (1-\eta-\eta^2)\eta_0^2\right]. \tag{23}$$

In Fig. 2 the function $\Phi_\alpha[\bar\eta(\alpha)]$ is plotted versus α for different values of the parameter η_0, while in Fig. 3 a comparison is displayed between the minimized energy and the result computed with the bulk penetration lengths $\xi_k/\sqrt{\alpha-1}$. It can be observed that the minimizing energy has a monotonic

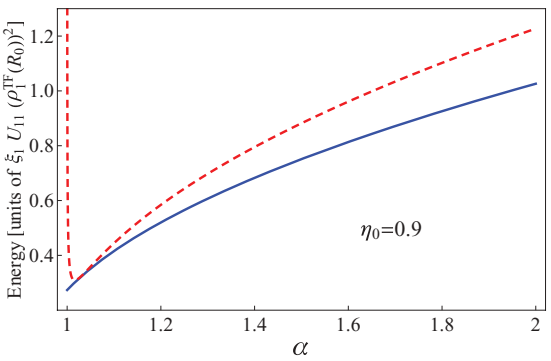

FIG. 3. (Color online) Comparison between the minimum energy $\{$units of $\xi_1 U_{11}[\rho_1^{\rm TF}(R_0)]^2\}$ of a domain wall [Eq. (21)] (solid blue line) and the energy computed for penetration lengths $\xi_k/\sqrt{\alpha-1}$, for $\eta_0 = 0.9$ (dashed red line).

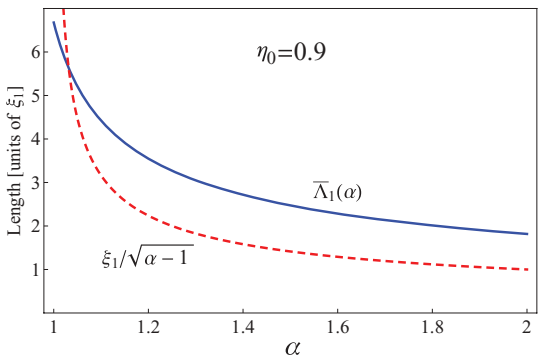

FIG. 4. (Color online) The solid (blue) line represents the optimal penetration length $\bar\Lambda_1(\alpha)$ (units of ξ_1) plotted against α for $\eta_0 = 0.9$. The dashed (red) line is the bulk penetration length $\xi_1/\sqrt{\alpha-1}$ [10], plotted here for comparison.

behavior with α. The optimal penetration length

$$\bar\Lambda_1(\alpha) = \xi_1\frac{\left(1+\frac{\eta_0^2}{\bar\eta(\alpha)}\right)}{\Phi_\alpha\left[\bar\eta(\alpha)\right]} \tag{24}$$

is plotted versus α (for $\eta_0 = 0.9$) in Fig. 4. The conditions ensuring that terms depending on the first derivatives of the densities can be neglected are thus summarized by the following inequality:

$$\frac{1+\eta_0^2/\bar\eta(\alpha)}{\Phi_\alpha[\bar\eta(\alpha)]}\frac{\hbar}{\sqrt{2m_1}}\frac{|V'(R_0)|}{U_{11}(\bar\rho_1)^{3/2}}\max_{j,k}\frac{\sqrt{U_{jj}}}{U_{kk}} \ll 1. \tag{25}$$

This condition also ensures that the distance between domain walls is always larger than Λ_k's, thus validating the results in Eqs. (15) and (16).

Since the dependence on α and $\rho_1^{\rm TF}$ in Eq. (21) is factorized, the total correction for a TF configuration with domain walls placed at $\{R_1, \ldots, R_w\}$ is

$$\Delta\mathcal{E}^{(w)} = \sum_{j=1}^{w}\mathcal{E}_{\rm wall}(R_j) \equiv C_\alpha\sum_{j=1}^{w}\left[\rho_1^{\rm TF}(R_j)\right]^{3/2}, \tag{26}$$

with

$$C_\alpha = \hbar(U_{11}/2m_1)^{1/2}\Phi_\alpha[\bar\eta(\alpha)]. \tag{27}$$

For confining potentials proportional to each other, including the interesting case in which they are equal, the energy increase Eq. (21) is independent of the specific domain wall, since Eq. (8) implies that the densities are the same at all the walls of a stationary configuration, namely, $\rho_1^{\rm TF}(R_j) = \rho_1^{\rm TF}(R_0)$ for any j [29]. This implies that the energy correction to a TF configuration with w domain walls is simply

$$\Delta\mathcal{E}^{(w)} = w\mathcal{E}_{\rm wall}(R_0). \tag{28}$$

On the other hand, the condition of applicability of our approximations in Eq. (25) depends on the specific domain wall through the first derivative of the potentials at each wall. Of course, a uniform control on the derivatives of the potentials would give a sufficient condition for their applicability to all possible configurations.

It should be emphasized that the validity of our approximation has an upper bound in α. Indeed, it can be deduced from Eq. (22) and Fig. 3 that the function $\Phi_\alpha[\bar\eta(\alpha)]$ is not bounded

from above as α increases, leading to a divergent correction to the TF energy, which frustrates regularization attempts. The reason lies in the fact that for $\alpha \to \infty$ the exponential tail ansatz is no longer justified, since in this case one species feels the other one like a hard wall, thus leading to solutions of the form $\tanh(x/\sqrt{2}\xi_k)$ and to a saturation of the domain-wall energy. Since the typical variation lengths of the densities are in this case $\sqrt{2}\xi_k$, we can bind the validity of our ansatz to values of α verifying $\bar{\Lambda}_k(\alpha) \lesssim \sqrt{2}\xi_k$ (see Fig. 4 for a comparison), typically corresponding to values $\alpha \lesssim 2.5$–3, which matches well the experimental ranges.

B. Profile edges

The presence of first-order zeros at the edges of the TF density profiles, which are compactly supported, gives rise to logarithmic divergencies in the kinetic energy. Even this situation can be tackled by a proper regularization of the densities, leading to an increase in the potential energy and to a kinetic contribution [17]. To this end, we consider a zero at position x_0 and conventionally consider a TF profile $\rho_k^{\mathrm{TF}}(x)\theta(x_0 - x)$ in a neighborhood of x_0, θ being the unit step function. The regularization is based on the solution of the linearized single-condensate wave function in a neighborhood of x_0, namely, $\sqrt{\rho_k} \propto \mathrm{Ai}(x/\delta)$, with $\mathrm{Ai}(y)$ being the proper Airy function [30], decreasing as $y \to \infty$, and

$$\delta_k = \left[\frac{2m_k F_k(x_0)}{\hbar^2}\right]^{-1/3}, \quad \text{with } F_k(x_0) = \left|\frac{dV_k}{dx}\right|_{x_0}, \tag{29}$$

being the characteristic length. Corrections to a solution based on the linear approximation of the potential are negligible if the second derivative of the potential is much smaller than $(2m_k F_k^4(x_0)/\hbar^2)^{1/3}$.

Following such a scheme, we consider the trial family of (continuous and positive) regularized TF profiles

$$\tilde{\rho}_k(x) = \begin{cases} \rho_k^{\mathrm{TF}}(x) & \text{if} \quad x < x_k \\ \rho_k^{\mathrm{TF}}(x_k)\, f\left(\frac{x-x_k}{\delta_k}\right)^2 & \text{if} \quad x \geqslant x_k \end{cases}, \tag{30}$$

with $f(y) = \mathrm{Ai}(y)/\mathrm{Ai}(0)$. As in the case of the domain wall, the point x_k is determined by requiring the local normalization condition to be fulfilled. The result, analogous to Eq. (12), reads

$$x_k - x_0 = -2I_0\delta_k, \tag{31}$$

where $I_0 = \int_0^\infty dy f^2(y) \simeq 0.53$. Summing the variations of the self-interaction energy (negative) and of the external potential energy (positive) to the kinetic energy yields the total-energy change due to the regularization of the zero of the density profile:

$$\mathcal{E}_{\mathrm{zero}}^{(k)}(x_0) \simeq 0.274\, \frac{\hbar^2}{m_k U_{kk}} F_k(x_0). \tag{32}$$

This contribution depends on the specific zero, as well as on the species k, since the first derivatives of the potential at its zeros are generally not related.

In order to get a feeling for the orders of magnitude of the various energies, one can consider the simple case in which the trapping potential is well approximated by a power law:

$$V(x) \sim |x|^n. \tag{33}$$

A TF zero, placed at x_0, of the density profile of species k, is determined by the condition $\mu_k = V(x_0) \sim x_0^n$. By considering the last relation and the normalization conditions, one can obtain the scaling law of the chemical potential with respect to the number of particles, namely, $\mu_k \sim N_k^{n/(n+1)}$. Hence one can obtain the scaling laws of the TF energy, $\mathcal{E}_{\mathrm{TF}} \sim N_k^{(2n+1)/(n+1)}$, and of the kinetic energy, including the contribution Eq. (32), $\mathcal{T} \sim N_k^{(n-1)/(n+1)}$. The energy of a domain wall depends on $(\rho^{\mathrm{TF}})^{3/2} \sim \mu^{3/2}$, and thus $\mathcal{E}_{\mathrm{wall}} \sim N_k^{3n/(2n+2)}$. The higher-order corrections of $\mathrm{O}(\bar{\Lambda}_k \rho_k'/\rho_k)$ terms accidentally scale like the kinetic energy. Thus, in a configuration with w domain walls, the trial ground state has energy

$$\mathcal{E} = \mathcal{U}_{\mathrm{TF}} + w\mathcal{E}_{\mathrm{wall}} + \mathrm{O}\left(N_k^{\frac{n-1}{n+1}}\right), \tag{34}$$

where

$$\mathcal{U}_{\mathrm{TF}} = \mathcal{E}_{\mathrm{TF}}\left(\rho_1^{\mathrm{TF}}, \rho_2^{\mathrm{TF}}\right) \tag{35}$$

is the energy of the TF densities.

IV. DOMAIN-WALL SUPPRESSION: A CASE STUDY

As an application of the previous results we consider in this section the energy crossing between configurations with different numbers of domain walls in a double-well potential. We will consider a physical situation in which a crossing between ground states with a maximal and a minimal number of domain walls can be observed. We introduce an operational way to control the crossing, based on a scaling property of the TF energy functional, thus suggesting a possible experimental realization.

Notice first that the effect of the kinetic energy on the ground state of a mixture in a square-well potential is trivial, since in this case the TF energy for separated configurations depends only on the volumes occupied by the two species and not on how they are distributed inside the well. Therefore, inclusion of the domain-wall energy immediately enables us to identify the configuration with a single domain wall as the ground state.

The situation is much more interesting for potentials that vary over the region occupied by the mixture. In the TF theory, density profiles with a maximal number of domain walls are usually energetically favored, especially when the ratio of the self-interaction coefficients is very close to 1 [29]. However, the inclusion of the kinetic energy can drastically change this picture. Each domain wall has an energetic cost, expressed by Eq. (21), whose effect on the total energy decreases as the numbers of particles increase. Thus, for very large number of particles, the ground state is more likely to have a maximal number of domain walls, but if the number of particles decreases or the parameter α increases it can become more convenient to reduce the number of walls.

As a test ground for the effectiveness of our method, let us consider an example of this phenomenon, that was analyzed by numerical integration of the coupled Gross-Pitaevskii stationary equations in Ref. [11]. The potentials are harmonic and the possible competing ground states have one or two walls: a mixture of ^{87}Rb atoms with $m_1 = m_2 = m = 1.45 \times 10^{-25}$ kg in two hyperfine states was considered, with scattering lengths $a_1 = 5.36$ nm and $a_2 = 5.66$ nm. The longitudinal

TABLE I. Total energy of a binary mixture of ^{87}Rb atoms in a harmonic potential with longitudinal frequency $\omega = 2\pi \times 90$ Hz and transverse frequency 30 times larger, for $N_1 = N_2 = 2000$ and $\alpha = 1.18$. The results obtained with the analytical approximation schemes proposed in this article are compared with those numerically obtained in Ref. [11].

	One wall (symmetry breaking)	Two walls (symmetry preserving)
$\mathcal{U}_{\rm TF}$	87.091	86.772
$\mathcal{E} = \mathcal{U}_{\rm TF} + \Delta\mathcal{E}^{(w)}$	87.486	87.423
$\mathcal{E}$ numerically computed in Ref. [11]	87.551	87.426

trapping frequency was fixed to $\omega = 2\pi \times 90$ Hz, with the transverse trapping frequency 30 times larger. The authors were able to build a phase diagram showing the crossing between single- and double-wall configurations by applying numerical techniques. An explicit comparison of the results for the total energies of the configurations is given in Ref. [11] for $N_1 = N_2 = 2000$ and $\alpha = 1.18$.

In Table I we compare our results with those of Ref. [11]. It is manifest that, while for the symmetry-preserving (double-wall) state the two results are identical up to the fourth significant digit, our regularization method enables us to attain a stricter upper bound for the ground-state energy of the symmetry-breaking (single-wall) configuration. Since the choice of the trial densities in the energy functional is based on the physics of the phenomenon, it is not surprising that our analytical regularization technique, together with the exact results coming from TF, leads to a better approximation of the ground state of a binary mixture than the accurate numerical integration of the coupled Gross-Pitaevskii equations [11].

The approximation on the energy of the trial densities was proved to be robust by a numerical check, in which the total energy of the regularized TF profiles is computed by numerical integration, showing only a slight increase in the fifth significant digit. The differences in the estimate of the ground-state energy of the symmetry-breaking configurations, which are general and not restricted to the aforementioned case, lead to a different phase diagram in the plane $(N_1 = N_2 = N, \alpha)$, shown in Fig. 5, that should be compared with that in Fig. 2 of [11]. In our case the transition line is shifted by a factor of $\simeq 1.5$ with respect to the N axis (towards larger values of N). Thus, according to our analysis, the symmetry-breaking ground state is present in a larger region of the (N, α) plane, where it was previously not expected.

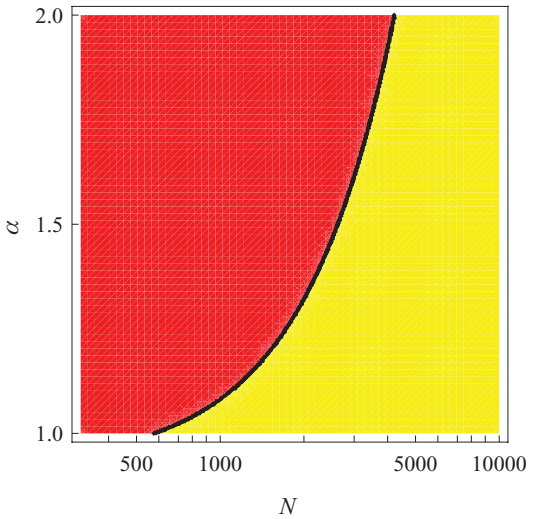

FIG. 5. (Color online) Ground-state phase diagram in the N-α plane for a binary mixture of ^{87}Rb atoms in a harmonic potential with longitudinal frequency $\omega = 90$ Hz and transverse frequency 30 times larger. In the light gray region (yellow in the online version) the ground state is a symmetry-preserving configuration with two domain walls, while in the dark gray region (red in the online version) a symmetry-breaking configuration, with a single domain wall, is energetically favored.

A. Scaling properties

It is convenient to study the scaling properties of the energy terms in Eq. (2) under a dilation. If lengths scale as $x \to x/a$ with $a > 0$, it is easy to see from Eqs. (3) and (4) that the kinetic energies scale as $\mathcal{T}_k \to \mathcal{T}_k/a$, while the potential and interaction energies scale as $\mathcal{V}_k \to a\mathcal{V}_k$ and $\mathcal{U} \to a\mathcal{U}$, and accordingly the numbers of particles scale as $N_k \to aN_k$. Therefore, the larger a and the numbers of particles, the smaller the ratio between kinetic and potential energy. Let us look at this property in more details.

Consider TF density profiles $\rho_k^{\rm TF}$ in a separated configuration given by Eq. (7) and fix their supports by choosing the number w of domain walls and their positions R_j, all satisfying $V(R_j) = v$ with v a constant value. Let the density profiles be normalized to N_k. The TF potential energy of the separated configuration reads

$$\mathcal{U}_{\rm TF}(N_k, V, w) = \sum_{k=1,2} \int_{\Omega_k} dx \left[V(x)\rho_k^{\rm TF}(x) + \frac{U_{kk}}{2}\rho_k^{\rm TF}(x)^2 \right]. \tag{36}$$

The integration domains $\Omega_k = \Omega_k(\{R_j\}, \{P_j^{(k)}\})$ are unions of intervals whose ends are domain walls or edges, located at $\{R_j\} = V^{-1}(\{v\})$ and $\{P_j^{(k)}\} = V^{-1}(\{\mu_k\})$, respectively. Observe now that, if the potential is scaled as

$$W(x) = V(x/a), \tag{37}$$

while leaving unchanged the chemical potentials μ_k and the domain-wall potential v, the density profiles $\sigma_k^{\rm TF}(x) = \rho_k^{\rm TF}(x/a)$ are still TF solutions, corresponding to the potential W, to supports $a\Omega_k = \Omega_k(\{aR_j\}, \{aP_j^{(k)}\})$, and to numbers of particles

$$\int_{a\Omega_k} dy\, \sigma_k^{\rm TF}(y) = a \int_{\Omega_k} dx \rho_k^{\rm TF}(x) = aN_k. \tag{38}$$

Moreover, the energy of the scaled configuration is related to the previous one by

$$\mathcal{U}_{\rm TF}(aN_k, W, w) = a\,\mathcal{U}_{\rm TF}(N_k, V, w). \tag{39}$$

On the other hand, the energy contribution of the domain walls is unchanged by the scaling, since it depends only on

fixed quantities, namely, the number of walls, the chemical potentials, and the domain-wall potential.

B. Energy crossing

Let us consider for definiteness a physical system with equal numbers N_0 of particles of the two species in a potential V, with w domain walls, potential energy $\mathcal{U}_{\rm TF}(N_0,V,w)$, and total domain-wall correction $\Delta\mathcal{E}^{(w)}$, proportional to w. If the numbers of particles are increased to $N = aN_0$ with $a > 1$ and the potential is stretched to $V(xN_0/N)$, the TF energy of the new configuration reads

$$\mathcal{U}_{\rm TF}\left(N, V\left(x\frac{N_0}{N}\right), w\right) = \frac{N}{N_0}\mathcal{U}_{\rm TF}(N_0, V(x), w), \qquad (40)$$

while the domain-wall contributions remain the same. We can conveniently consider N_0 such that the bulk kinetic energy and the energy corrections due to the zeros of the density profiles are negligible with respect to both the TF energy and the domain wall energy. *A fortiori*, they will be negligible for all $N > N_0$, since the bulk kinetic energy scales like N_0/N.

We consider now an alternative configuration, in which the number of domain walls is w'. The potential energy $\mathcal{U}_{\rm TF}(N, V(xN_0/N), w')$ obeys the same scaling law [Eq. (40)]. If a crossing between the total energies of the configurations exists, it occurs for a number of particles

$$N^*_{w,w'}(\alpha) = N_0\frac{\Delta\mathcal{E}^{(w)}(\alpha) - \Delta\mathcal{E}^{(w')}(\alpha)}{\mathcal{U}_{\rm TF}(N_0, V(x), w') - \mathcal{U}_{\rm TF}(N_0, V(x), w)}, \qquad (41)$$

which is meaningful only if the differences of the potential energies and of the domain wall-corrections have opposite signs. Furthermore, physical meaning can be attributed to the crossing only if $N^*_{w,w'} \geqslant N_0$, since the validity of TF approximation is not assured for $N < N_0$.

Binary mixtures of ^{87}Rb atoms are experimentally available [5,9], with mass $m_1 = m_2 = m = 1.45 \times 10^{-25}$ kg, in states $|F = 1, m_F = +1\rangle$ and $|F = 2, m_F = -1\rangle$, whose s-wave scattering lengths are, respectively, $a_1 = 5.36$ nm and $a_2 = 5.66$ nm. The interspecies scattering length a_{12} is tunable by approaching a Feshbach resonance [31] (see [4,5,9] for experimental realizations). Let us suppose that such a mixture is confined in a deformed harmonic trap, with a longitudinal frequency $\omega_\ell = 2\pi \times 0.7$ Hz, corresponding to a trapping length $a_\ell = \sqrt{\hbar/(m\omega_\ell)} = 1.29 \times 10^{-5}$ m and a transverse frequency $\omega_\perp = 500\,\omega_\ell$, such that $a_\perp = a_\ell/(10\sqrt{5})$. Since we want the transverse degrees of freedom to be frozen, the number of particles per species N_0 has to satisfy $N_0 \ll a_\ell^2/(a_\perp \min(a_1, a_2)) \simeq 5 \times 10^4$. Moreover, in order to ensure the applicability of one-dimensional TF approximation, the condition $N_0 \gg a_\perp^2/(a_\ell \max(a_1, a_2)) \simeq 10$ must hold [17]. A good choice is then $N_0 = 5 \times 10^3$. It is readily verified that if the potential is (longitudinally) scaled as in Eq. (37), the assumption of one-dimensionality and the TF approximation continue to be valid. The one-dimensional self-interaction parameters read

$$U_{kk} = \frac{2\hbar^2 a_k}{m_k a_\perp^2}, \qquad (42)$$

and their ratio $U_{11}/U_{22} = a_1/a_2$ is very close to 1.

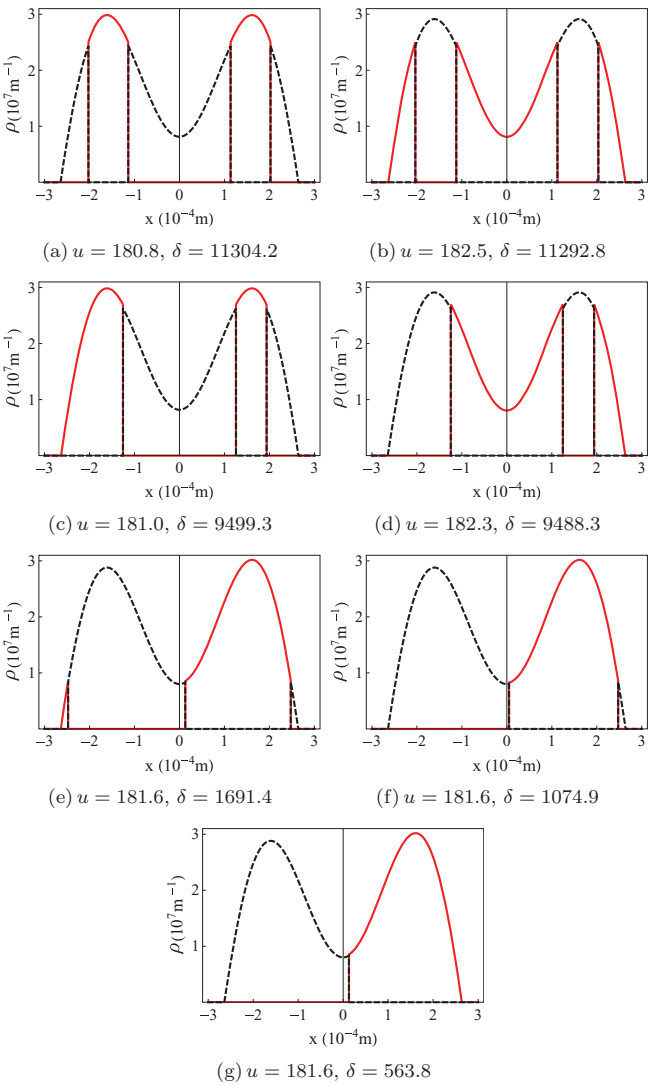

(a) $u = 180.8$, $\delta = 11304.2$ (b) $u = 182.5$, $\delta = 11292.8$

(c) $u = 181.0$, $\delta = 9499.3$ (d) $u = 182.3$, $\delta = 9488.3$

(e) $u = 181.6$, $\delta = 1691.4$ (f) $u = 181.6$, $\delta = 1074.9$

(g) $u = 181.6$, $\delta = 563.8$

FIG. 6. (Color online) Lowest-energy configurations in the double-well potential Eq. (43), for $N_0 = 5 \times 10^3$ and $\alpha = 2$. In all figures the (linear) densities of species 1 (solid red line) and species 2 (black dashed line) are plotted vs the linear coordinate x. Below each figure, $u = \mathcal{U}(N_0, V, w)/N_0$ is the TF potential energy per particle, while δ is the specific energy of the domain walls as in Eq. (26), both in units $\hbar\omega_\ell$.

In order to obtain a double well in the region where the condensates are trapped, we add to the longitudinal harmonic potential a cosine potential, so that

$$V(x) = \frac{m\omega_\ell^2}{2}x^2 + A\cos(Bx), \qquad (43)$$

with $A/(\hbar\omega_\ell) = 107.75$ and $Ba_\ell = 6.44 \times 10^{-16}$.

The TF stationarity condition Eq. (8), together with the normalization conditions, is satisfied by the seven different configurations represented in Fig. 6, together with their TF and domain-wall energies. The number of domain walls ranges from 1 to 4. The configuration with four domain walls and with the less-self-interacting species placed in the minima of the external potential is, as expected, the minimizer of the TF energy. However, its domain-wall energy is much larger than that of the configuration with a single domain wall, where each

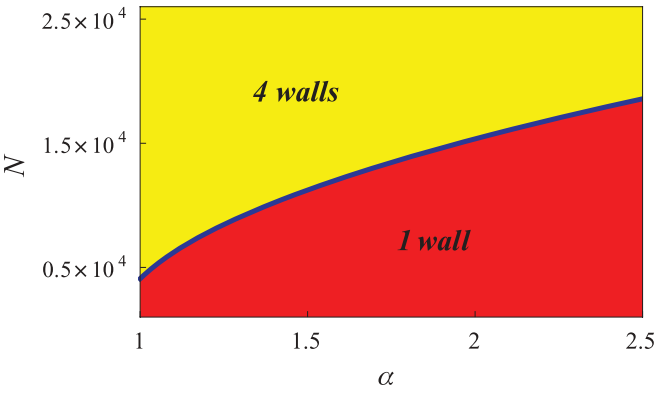

FIG. 7. (Color online) Ground-state phase diagram for a mixture with equal number of atoms $N_1 = N_2 = N$ in the potential $V(x)$ of Eq. (43). In the light gray region (yellow in the online version) configurations with the maximal number of walls are energetically favored, while in the dark gray region (red in the online version) the ground state has a single domain wall. The (blue) transition line represents the function $N^*_{1,4}(\alpha)$.

condensate occupies one well. For instance, $\alpha = 2$ yields, according to definition Eq. (41), $N^*_{1,4}(2) = 1.4 \times 10^4$. We have observed that for all α the only competing ground states are the aforementioned configurations, with one and four domain walls. The four-wall profile is the ground state only for $N > N^*_{1,4}(\alpha)$, while for smaller N the one with a single domain wall is energetically favored. In Fig. 7 the ground-state phase diagram is displayed. The transition line is the graph of the function

$$N^*_{1,4}(\alpha) \propto \Phi_\alpha[\bar{\eta}(\alpha)] \tag{44}$$

and gives direct information about the function $\Phi_\alpha[\bar{\eta}(\alpha)]$. Thus, using Eqs. (21) and (24), the ground-state phase diagram can be used to obtain information about the domain-wall energies and the optimal penetration lengths.

V. CONCLUSIONS AND OUTLOOK

We discussed a variational method that yields a very good approximation for the total energy of a binary mixture of Bose-Einstein condensates in a separated configuration. The method is reliable and accurate. We have seen that, in some cases, density profiles with a large number of domain walls can be energetically favored with respect to those with fewer domain walls, in particular when the interaction ratio α is close to 1. At present, there is a variety of methods to find approximate solutions to the Gross-Pitaevskii equations, ranging from analytical techniques [32] to numerical ones, including imaginary-time schemes [33,34] and finite-difference methods [35–37]. It is worth emphasizing that our approach is not aimed at solving the Gross-Pitaevskii equations in the most general cases, but is rather optimized at uncovering the ground-state properties of the mixture, with minimal numerical help. This enables us to give an immediate physical interpretation of the results and makes it possible to explain in very general terms the observed phenomena, to predict new ones, and possibly to develop more refined techniques in order to extend the validity of our approximations.

All results are analytical and therefore provide solid ground to improve the approximations. Indeed, starting from Eq. (21) and from previously obtained TF results [29], it is possible to compute, for example, corrections due to the first (finite) derivatives of the potentials, as well as possible domain-wall displacements and small variations of the chemical potentials.

The results obtained in this paper can have practical applications. For example, if one compares an experimental phase diagram with the theoretical prediction, physical properties of the mixture can be estimated from the transition line, that depends on the ratio of the masses and the interaction parameters. These results can also help in analyzing dynamical phenomena, such as vortices and solitons, which mostly appear as perturbations of a stationary background, and lead to very subtle energy changes (see, e.g., [16,38,39]): in order to correctly analyze these changes, an accurate estimate of the background energy is needed.

[1] T. L. Ho and V. B. Shenoy, Phys. Rev. Lett. **77**, 3276 (1996).
[2] A. J. Leggett, Rev. Mod. Phys. **73**, 307 (2001).
[3] A. Görlitz, J. M. Vogels, A. E. Leanhardt, C. Raman, T. L. Gustavson, J. R. Abo-Shaeer, A. P. Chikkatur, S. Gupta, S. Inouye, T. Rosenband, and W. Ketterle, Phys. Rev. Lett. **87**, 130402 (2001).
[4] C. J. Myatt, E. A. Burt, R. W. Ghrist, E. A. Cornell, and C. E. Wieman, Phys. Rev. Lett. **78**, 586 (1997).
[5] D. S. Hall, M. R. Matthews, J. R. Ensher, C. E. Wieman, and E. A. Cornell, Phys. Rev. Lett. **81**, 1539 (1998).
[6] G. Modugno, M. Modugno, F. Riboli, G. Roati, and M. Inguscio, Phys. Rev. Lett. **89**, 190404 (2002).
[7] G. Thalhammer, G. Barontini, L. De Sarlo, J. Catani, F. Minardi, and M. Inguscio, Phys. Rev. Lett. **100**, 210402 (2008).
[8] S. B. Papp, J. M. Pino, and C. E. Wieman, Phys. Rev. Lett. **101**, 040402 (2008).
[9] S. Tojo, Y. Taguchi, Y. Masuyama, T. Hayashi, H. Saito, and T. Hirano, Phys. Rev. A **82**, 033609 (2010).
[10] P. Ao and S. T. Chui, Phys. Rev. A **58**, 4836 (1998).
[11] K. Kasamatsu, Y. Yasui, and M. Tsubota, Phys. Rev. A **64**, 053605 (2001).
[12] M. Trippenbach, K. Góral, K. Rzążewski, B. Malomed, and Y. B. Band, J. Phys. B **33**, 4017 (2001).
[13] Yu. G. Gladush, A. M. Kamchatnov, Z. Shi, P. G. Kevrekidis, D. J. Frantzeskakis, and B. A. Malomed, Phys. Rev. A **79**, 033623 (2009).
[14] N. Suzuki, H. Takeuchi, K. Kasamatsu, M. Tsubota, and H. Saito, Phys. Rev. A **82**, 063604 (2010).
[15] D. Kobyakov, V. Bychkov, E. Lundh, A. Bezett, V. Akkerman, and M. Marklund, Phys. Rev. A **83**, 043623 (2011).
[16] S. Gautam, P. Muruganandam, and D. Angom, J. Phys. B **45**, 055303 (2012).

[17] L. Pitaevskij and S. Stringari, *Bose-Einstein Condensation* (Clarendon, Oxford, 2003).
[18] Y. Hao, Y. Zhang, X. W. Guan, and S. Chen, Phys. Rev. A **79**, 033607 (2009).
[19] S. Gautam and D. Angom, J. Phys. B **44**, 025302 (2011).
[20] S. Gautam and D. Angom, J. Phys. B **43**, 095302 (2010).
[21] F. Riboli and M. Modugno, Phys. Rev. A **65**, 063614 (2002).
[22] A. K. Kolezhuk, Phys. Rev. A **81**, 013601 (2010).
[23] E. Timmermans, Phys. Rev. Lett. **81**, 5718 (1998).
[24] R. A. Barankov, Phys. Rev. A **66**, 013612 (2002).
[25] I. E. Mazets, Phys. Rev. A **65**, 033618 (2002).
[26] B. Van Schaeybroeck, Phys. Rev. A **78**, 023624 (2008).
[27] A. L. Fetter and J. D. Walecka, *Quantum Theory of Many-Particle Systems* (McGraw-Hill, New York, 1971).
[28] E. H. Lieb, R. Seiringer, and J. Yngvason, Phys. Rev. A **61**, 043602 (2000).
[29] P. Facchi, G. Florio, S. Pascazio, and F. V. Pepe, J. Phys. A **44**, 505305 (2011).
[30] M. Abramowitz and I. A. Stegun, *Handbook of Mathematical Functions: With Formulas, Graphs, and Mathematical Tables* (Dover Publications, New York, 1965).
[31] H. Feshbach, Ann. Phys. (NY) **5**, 337 (1958).
[32] H. Salman, Phys. Rev. A **85**, 063622 (2012).
[33] S. Palpacelli, S. Succi, and R. Spigler, Phys. Rev. E **76**, 036712 (2007).
[34] D. Baye and J.-M. Sparenberg, Phys. Rev. E **82**, 056701 (2010).
[35] A. Gammal, T. Frederico, and L. Tomio, Phys. Rev. E **60**, 2421 (1999).
[36] M. M. Cerimele, M. L. Chiofalo, F. Pistella, S. Succi, and M. P. Tosi, Phys. Rev. E **62**, 1382 (2000).
[37] S. K. Adhikari, Phys. Rev. E **63**, 056704 (2001).
[38] A. Balaž and A. I. Nicolin, Phys. Rev. A **85**, 023613 (2012).
[39] P. Kuopanportti, J. A. M. Huhtamäki, and Mikko Möttönen, Phys. Rev. A **85**, 043613 (2012).